Available online at www.sciencedirect.com
ScienceDirect
Physics and Chemistry of the Earth 32 (2007) 820–831
PHYSICS and CHEMISTRY of the EARTH
www.elsevier.com/locate/pce

Hydromechanical study of rock–mortar interfaces

O. Buzzi [a,*], J. Hans [a], M. Boulon [a], F. Deleruyelle [b], F. Besnus [b]

[a] *Laboratoire "Sols, Solides, Structures" UMR 5521, Université Joseph Fourier, Grenoble, France*
[b] *Institut de Radioprotection et Sûreté Nucléaire, Fontenay aux roses, France*

Received 30 March 2005; received in revised form 12 March 2006; accepted 12 March 2006
Available online 16 October 2006

Abstract

Hydromechanical compression tests have been performed on rock–mortar interfaces representing the contact between a host rock and a concrete bulkhead within an underground nuclear waste repository. The rock used in the tests is a Toarcian argillite. Most published studies concerning rock–concrete interfaces involve concrete–concrete contacts in which rock replicas are used instead of real rock samples. As a result, the effect of rock features, such as bedding planes and changes of the rock interface zone, on the hydromechanical behaviour of the interface cannot be investigated. The tests discussed in this paper demonstrate that the mechanical response is not affected when changing the parameters of the samples even not mismatching both walls. On the contrary, an initial monitored lateral displacement modifies the hydromechanical behaviour by limiting the interface ability to be hydraulically closed. The latter ability has been quantified by a simple evolution law and the difference of behaviour between the two kinds of samples has been confirmed. The analysis led to determine the hydraulic aperture shows that the values obtained are much lower to the classical values available in the literature. Finally, the application of the experimental results to the confinement by a bulkhead showed the localization of the flow within the interface.

Keywords: Interface; Argillite; Mortar; Transmissivity; Hydromechanical behaviour; Compression; Hydraulic aperture

1. Introduction

Disposal in underground geological repositories has been selected in many countries (Canada, France, Sweden, Spain, Japan and others), as the method for isolating nuclear waste from the biosphere. Repository design relies on natural and engineered barriers for confinement of the waste. Underground Research Laboratories (URL's) have been developed in a number of these countries to study the feasibility of underground isolation. Although the physical properties of most of the materials involved (rock, concrete and bentonite mixtures) are now reasonably well known, there have been few studies to date on the behaviour of the contact interfaces between these materials. Observations during Tunnel Sealing experiment (Dixon et al., 2002) have indicated that any flow that was able to 'escape' past the tunnel seal when fluid pressure was applied to the inner surface of the sealed was localized within the contact interface between the host rock and the seal barrier. This observation has drawn attention to the fact that the behaviour of interfaces may be critical in determining the effectiveness of an engineered barrier.

Studies have been conducted on rock–bentonite interfaces by Gens et al. (2002), Grindrod et al. (1999), Pusch (1983) and Dixon et al. (2002), but very little is available on real rock–concrete interfaces, despite their relevance for nuclear waste disposal, dam stability or other soil-(or rock-) structure interactions. Usually, such contacts are considered to behave in the same way as rock joints. When they are investigated, artificial rock or mortar replicas of the surfaces are often used (Johnston and Kodikara, 1994; Johnston and Lam, 1984; Seidel and Haberfield, 2002). As a result, while roughness can be simulated easily (Seidel and Haberfield, 2002), some rock parameters, such

* Corresponding author. Fax: +33 4 76 82 70 00.
E-mail address: olivier.buzzi@hmg.inpg.fr (O. Buzzi).

1474-7065/$ - see front matter © 2006 Elsevier Ltd. All rights reserved.
doi:10.1016/j.pce.2006.03.010

as natural discontinuities of the bedding planes – which can constitute a pathway for water and increasing the transmissivity of the interface – cannot be reproduced using replicas.

This study deals with the contact between the host shale rock (argillite) and a concrete bulkhead, represented at the laboratory scale by mortar–argillite interfaces. This shale rock is highly anisotropic (Rejeb (1999)) because of the bedding planes. The influence of bedding planes on the hydromechanical behaviour has been investigated. Other parameters relevant to the in situ configuration of the concrete bulkhead have also been investigated. Mortar–rock interfaces are formally very similar to rock joints, so similar hydromechanical behaviour can be expected (Gangi, 1978; Benjelloun, 1991; Lee and Cho, 2002; Hans and Boulon, 2003). Our series of experiments is focussed on the influence of some sample parameters on the intrinsic transmissivity when a compressive load is applied across the interface. Since the argillite is very sensitive to hydration/dehydration (Charpentier et al., 2003), particular attention has been paid to any modification of the rock within the interface zone due to water and normal stress.

This paper presents the experimental results obtained on the hydromechanical behaviour of rock–mortar interfaces. Results are interpreted in terms of intrinsic transmissivity and of the 'hydraulic aperture' – a concept often used in the analysis of the flow of fluids through rock fractures (Barton et al., 1985; Boulon et al., 1993; Esaki et al., 1999; Olsson and Barton, 2001). A simple application of the experimental results to a full-scale configuration is proposed.

2. Experimental facilities

The tests were performed using the direct shear box BCR3D and the associated hydraulic device. This apparatus was designed by Boulon (1995) and developed by Armand et al. (2000) and Hans (2002).

2.1. The direct shear box BCR3D

This experimental device enables all classical compression tests and shear tests (constant normal stress, constant stiffness, constant volume) and has a shear velocity ranging from 0.05 mm/s to 50 cm/s through the use of both quasi-static and dynamic electro-mechanical jacks. The BCR3D has been designed to avoid any relative rotation of the rock walls during the shear displacement. Such a relative rotation can affect greatly the quality of the tests (Boulon, 1995). By the use of two actuators on the horizontal shear axis, the relative tangential displacement of both rock walls are symmetrical with respect to the vertical axis allowing the application of the normal force on the joint. One advantage is that the normal force is kept centered on the active surface of the joint preventing the upper part of the sample from rotating. Each axis is equipped with one or two actuators (capacity of 100 kN) and of sensors measuring displacement and force. Two LVDT's are used on the normal load axis to check that there is no parasite rotation during the shear test. A front cross-sectional view of the apparatus is shown in Fig. 1. For the experiments described in this paper, the BCR3D was used in compression only.

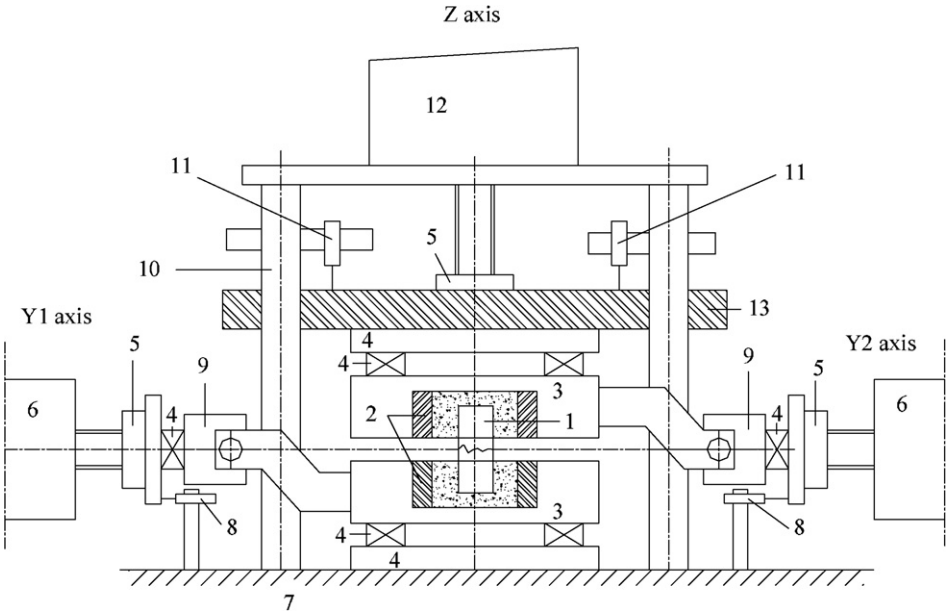

Fig. 1. Front view section along one shear axis of the BCR3D: (1) sample to be tested, (2) internal removable metallic boxes, (3) external boxes, (4) specific device enabling translation movements, (5) load cells, (6) horizontal actuators, (7) rigid frame, (8) displacement sensors (LVDT measuring Δy_1 and Δy_2), (9) coupling device, (10) rigid columns, (11) displacement sensors (LVDT measuring Δz and δz), (12) vertical actuator, (13) rigid vertically translating structure.

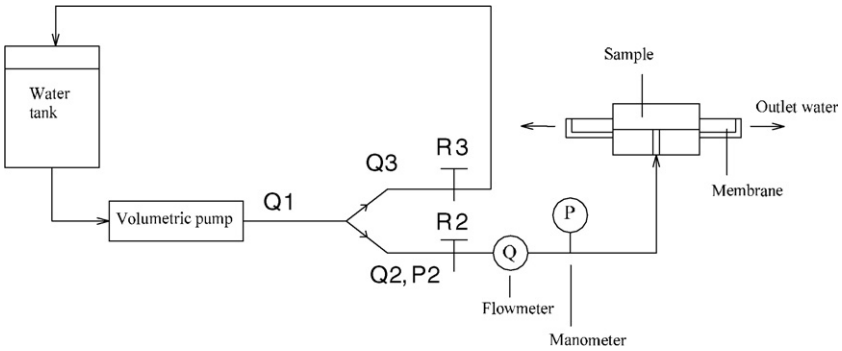

Fig. 2. Diagram of the hydraulic device. The pump injects a constant flow rate (Q1) into the circuit which is divided into two branches. One branch (Nr3) is the discharge whereas the other one (Nr2) goes to the sample with a continuous measurement of flow rate and of pressure.

2.2. The associated hydraulic device

The diagram of the hydraulic device used for the hydro-mechanical tests is shown in Fig. 2. A constant water flow Q1 produced by the volumetric pump is injected into the hydraulic circuit which is divided in two branches: the first one (Nr3) is an adjustable discharge. The second branch (Nr2) is connected to the sample with a continuous measurement of the pressure (P2) and the flow rate (Q2). Both hydraulic gates R2 and R3 are used to drive the test which is neither at constant injection pressure nor at constant flow rate. The outlet water (at atmospheric pressure) is collected by a membrane.

2.3. Materials

The rock used is an argillite of the Toarcian age from the IRSN experimental site of Tournemire. Many studies have been led on this material (Niandou et al., 1997; Daupley, 1997; Mathieu et al., 2000; Rejeb, 1999). This rock has a high clay fraction (70% of clay (kaolinite, illite, smectite, mica), from 10% to 20% of calcite and from 10% to 20% of quartz), is saturated in its natural state and is highly anisotropic (due to the bedding planes). Some mechanical data about the intact rock are available in Rejeb (1999). The modulus of elasticity ranges from 9 GPa to 32 GPa depending on the location of the site from which the rock sample was taken. The water content is very low (from 1% to 5%) as for the permeability (from 10E−13 to 10E−15 m/s) (from Rejeb, 1999).

The Rapidex 712 Mortar from Lanko has been used to prepare the mortar part of the interface. Some tests performed at the laboratory gave an unixial compressive strength of 35 MPa at 24 h and a tensile strength of 6 MPa at 24 h. The Young's modulus is about 15 GPa.

2.4. Specimen preparation

A different rock sample was used for each hydromechanical test in order to highlight any modification of the rock and any possible influence of the stratification (natural discontinuity of the rock) on the evolution of the transmissivity of the interface. However, to compare results, the rock wall morphology must be constant. This was achieved by creating an artificial roughness, which was reproducible. The regular grooves were made by hand with a saw before sealing the sample to create the contact – as shown in Fig. 3. The procedure followed to prepare the interface samples, so as to allow radial flow, is explained in Fig. 4.

2.5. Experimental program

2.5.1. Parameters studied

Fig. 5 gives a general view of the variables considered in this study. Let us consider a geological massif with a specific orientation of the bedding planes (here horizontal) in which a gallery is excavated. In case of a concrete bulkhead poured in place, the natural shrinkage of the concrete can lead to either a distinct aperture at the interface (Didry et al., 2000) or at least to a reduction in the compression

Fig. 3. Artificial roughness of the rock wall: hand made grooves (section 1 mm per 1 mm, diameter of the sample 63 mm).

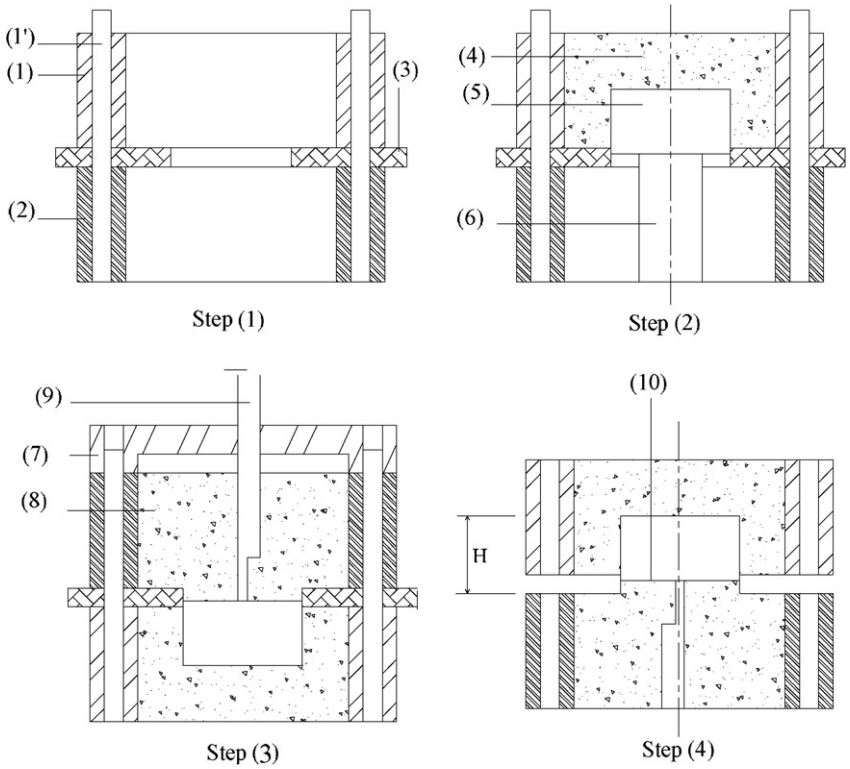

Fig. 4. Diagram of specimen preparation. Step 1: metallic boxes (1) and (2) and the complementary mould (3) are assembled using the pins (1′). Step 2: the rock sample (5) is positioned using a wedge (6) and sealed with a mortar (4). Step 3: The specific device for the centered injection hole ((7) and (9)) is positioned and the mould is filled with mortar (8). Step 4: after a few hours, all pieces are removed and the interface sample (10) can be tested. *H*: height used to calculate the Young's modulus.

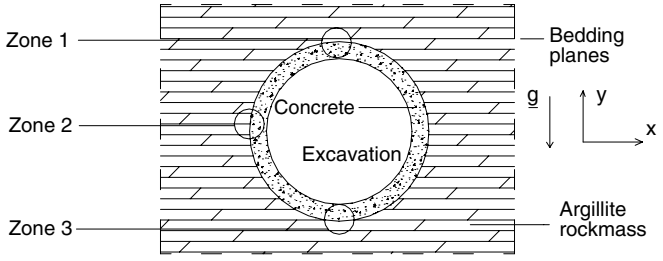

Fig. 5. Diagram of a geological massif of specific bedding planes in which a gallery is excavated and a concrete structure is built.

across the interface. The long term convergence of the excavation due to rock creep will progressively compress the interface, tending to close it. However, the different zones of contact between the host rock and the bulkhead do not follow the same history.

The bottom (zone 3) should not be opened (except in case of ovalization of the gallery). The vault (zone 1) may be opened and closed without any lateral relative displacement (symmetrical geometry) whereas any other zone (e.g. zone 2) will be closed with a small tangential relative displacement between the rock wall and the concrete (called lateral displacement). Moreover, the orientation of the bedding planes with regards to the contact plane differs from one zone to another. The orientation of the contact plane with regards to the gravity may also have an importance since segregation and laitance phenomena usually occur when pouring concrete (Neville, 2000). Thus, we will distinguish two configurations (to reduce the number of combination of the parameters): the contact plane can be seen as the bottom (zone 3) or the side of the concrete mould (zone 2).

Table 1 outlines a suite of tests with different combinations of the variables. The 14 samples have each been loaded following a prescribed loading path. The in situ stress ranges from about 11 MPa to about 15 MPa

Table 1
Set of the tests performed

Tests	1AM	2AM	3AM	4AM	5AM	6AM	7AM
Stratification	PA	PA	PA	PE	PE	PE	PE
Mould	B	B	B	B	B	S	S
History	O	LD	LD	O	NO	O	LD
	8AM	9AM	10AM	11AM	12AM	13AM	14AM
Stratification	PA	PA	PA	PA	PE	PE	PE
Mould	B	B	S	S	B	B	S
History	NO	NO	NO	NO	O	LD	LD

Meaning of the symbols: the stratification can be parallel (PA) or perpendicular (PE) to the contact plane. The interface can be seen as the bottom (B) or the side (S) of the concrete mould. The contact may have been never opened (NO), opened and closed without any lateral displacement (O) or opened and closed with a lateral displacement of 1 mm (LD).

(ANDRA, 2001) but, as noted previously, the final stress depends on the behaviour of the sample and on the experimental device. The actual stresses in the tests ranged from 5 MPa to 21 MPa.

2.5.2. Test procedure

After installing the sample in the experimental device and preparing it for testing, an initial normal stress of 1 MPa is applied. Flow is then started and the steady-state pressure and flow rate monitored continuously. The total normal stress is increased progressively from 1 MPa to 1 MPa with steps of hydraulic steady state measurement. The final normal stress depends on the sample behaviour and any technical problems such as leakage.

From a hydraulic point of view, changes in the initial flow rate and pressure are the result of compression of the interface only. However, if the flow rate is too small to be measured, the operator can increase the rate in order to continue the test and to obtain relevant data. It should be noted the all of the tests carried out involve compression loading of the sample.

2.5.3. Calculation of the hydraulic transmissivity

As with rock joints, the argillite–mortar interfaces are networks of voids, of overall permeability k, saturated with water and following Darcy's law. The transmissivity tests are performed on annular specimen of interface. A quasi-radial permanent flow is created by applying an injection overpressure of fluid ΔP at the internal radius (r_i) of the sample, and atmospheric pressure (taken to be the pressure origin) at the external radius (r_e) of the sample (see Fig. 6). As with many other investigators (Hans and Boulon, 2003; Esaki et al., 1999; Lee and Cho, 2002), the test results have been interpreted in terms of transmissivity rather than permeability because this avoids the necessity to make a hypothesis for the local hydraulic aperture. Assuming that the transmissivity of the interface is isotropic, the intrinsic transmissivity T can be expressed as

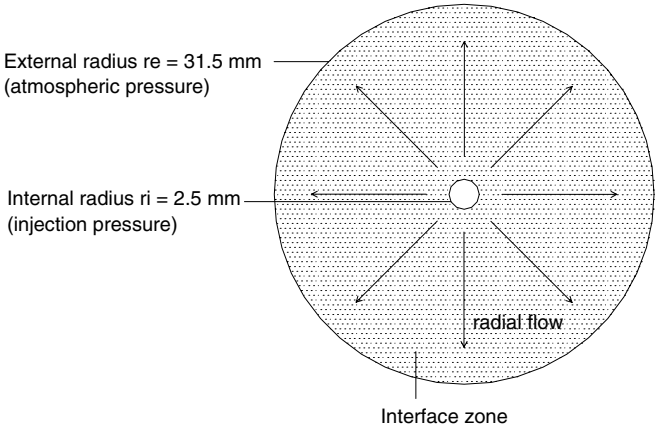

Fig. 6. Annular geometry of the interface and radial flow.

$$T = \frac{\ln(r_e/r_i)}{2\pi} \cdot \mu \cdot \frac{Q}{\Delta P} \quad (1)$$

with:

- T: intrinsic transmissivity (m^3),
- Q: flow rate (m^3/s),
- ΔP: internal injection pressure (Pa),
- r_e: external radius of the annular sample (mm),
- r_i: internal radius (mm),
- μ: dynamic viscosity of the fluid (Pa s).

As for permeability, the transmissivity t and the intrinsic transmissivity T are linked by $T = t \cdot \frac{\mu}{\gamma_w}$ with γ_w: weight density of the fluid (N/m^3).

The intrinsic transmissivity is used to express the results independently of the fluid properties. The temperature of the fluid having an influence on its viscosity has been measured during the whole campaign and it varies very slightly (from 18 °C to 21 °C). Its incidence on the transmissivity calculation has thus been neglected.

3. Results

3.1. Mechanical responses

It is well known that a discontinuity affects the stiffness of the rock matrix and that the effect is greater if the joint is mismatched (Bandis et al., 1983). We have therefore separated the results of matched and mismatched interfaces (i.e. without and with lateral displacement respectively). Fig. 7

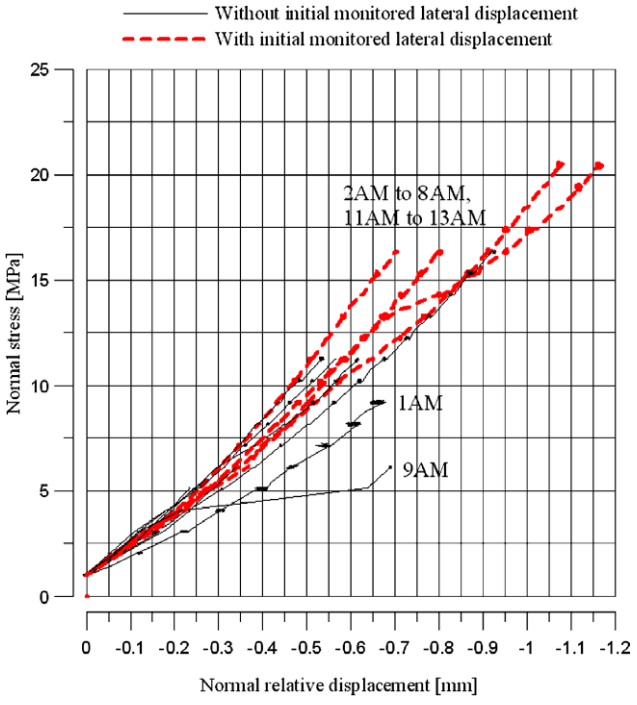

Fig. 7. Evolution of normal stress with respect to normal relative displacement for mechanical compression tests on argillite–mortar interfaces.

shows the change in normal stress σ_n with normal relative displacement for all the tests. It should be noticed that the mechanical responses are very similar (except for tests 1AM and 9AM). This indicates that the test variables had no major influence on the mechanical response of the samples. The average initial normal stiffness of the samples calculated from the mechanical response Fig. 7 is about 16 MPa/mm. Even when the strains are not homogeneous, we can calculate a maximum value for the global modulus of elasticity. The sealing mortar ((4) and (8)) cannot slip from the metal boxes ((1) and (2)) (see Fig. 4) and assuming that only the part of the sample of lower section is strained (i.e. the whole rock sample and the 63 mm diameter mortar part see Fig. 4), we can establish a maximum value for the global modulus of elasticity of the sample:

$$E_{\text{global}} = k_n \cdot H \tag{2}$$

with H: height of the sample argillite part added to the mortar part of lower section (see Fig. 4). The maximum value is obtained for the highest sample (65 mm theoretically). This leads to a value of:

$$E^{\max}_{\text{global}} = k_n \cdot H_{\max} = 1.12 \text{ GPa}$$

The modulus of elasticity of the rock and of the mortar are greater than 9 GPa and approximately 15 GPa respectively. The global modulus of elasticity of the samples is thus affected considerably by the discontinuity. However, contrary to the qualitative results by Bandis et al. (1983), we do not observe any difference in stiffness between well matched samples (with no initial lateral displacement) and mismatched samples (with an initial lateral displacement). This is probably due to the very smooth character of the walls.

3.2. Hydromechanical responses

Fig. 8 shows the change in transmissivity (on a semi-logarithmic scale) with normal stress for all the tests (except 10AM and 14AM, which failed). Unlike the mechanical responses, the curves are much more dispersed and the change in transmissivity differs from one sample to another. First, there is a natural initial dispersion due to hydraulic conditions and rock wall morphology which are not exactly the same for all of the tests. There are almost two orders of magnitude of dispersion under a normal stress of 1 MPa ($T = 1\text{E}{-16}\ \text{m}^3$ for test 11AM and $T = 6\text{E}{-15}\ \text{m}^3$ for test 6AM). This dispersion increases with increase in the normal stress.

For all the tests, the transmissivity decreases with increase in normal stress. This classical result of rock mechanics is due to the reduction of voids and increase in tortuosity (Hans and Boulon, 2003; Lee and Cho, 2002; Gale and Raven, 1985; Capasso et al., 1999). However, the manner in which the transmissivity decreases is different for each test. Samples without initial lateral displacement seems to close sooner (i.e. at a lower normal stress) than those with an initial lateral displacement. Complete hydraulic closure of the interface (flow equal to zero) but with residual electronic noise leads to an approximate value of transmissivity of about $1\text{E}{-19}\ \text{m}^3$ that can be detected for tests 5AM, 8AM, 11AM and 12AM. Concerning test 12AM, complete hydraulic closure appeared to be developing but an unexpected leakage ended the test.

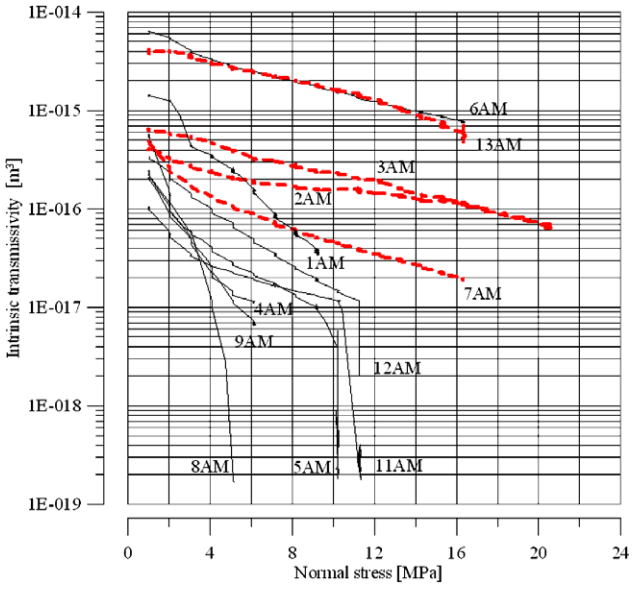

Fig. 8. Evolution of intrinsic transmissivity with respect to normal stress.

The influence of stratification can be assessed from tests 4AM, 5AM, 6AM and 12AM which have a bedding plane orientation perpendicular to the contact plane and no lateral displacement (see Table 1). The existing discontinuities may allow some water flow, thereby increasing the transmissivity of the interface. In fact it is observed that it is not the case since the transmissivities are very low (except for test 6AM) and hydraulic closure is reached. This suggests that orientation of stratification has no significant influence on the hydromechanical behaviour of such interfaces when subjected to compression. Finally, except for some local damage due to normal stress (which is to be expected), the rock appeared to be unchanged at the end of the hydromechanical tests.

4. Discussion

4.1. Influence of the initial lateral displacement

Analysis of the results indicates that the test variables have no major influence on the mechanical behaviour of the interface. Lateral displacement alone has any influence on the fluid transmissivity of the interface. In order to confirm this conclusion, we have investigated the change in relative transmissivity, Fig. 9, represented by the factor θ as a function of the normal stress This allows us to examine the evolution of the transmissivity independently of the initial dispersion. θ is defined as follows:

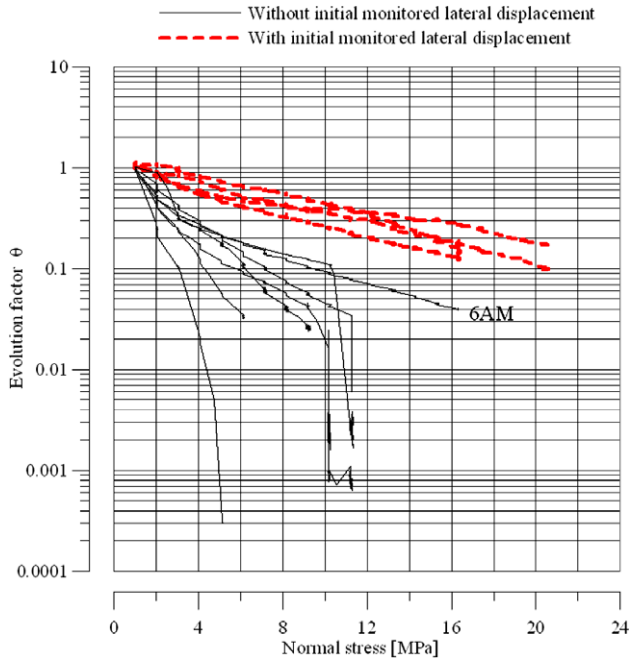

Fig. 9. Evolution factor θ as a function of normal stress σ_n. θ is defined by $T(\sigma_n, \Delta P, Q) = \theta(\sigma_n, \Delta P, Q) \cdot T_1^{max}$ with T_1^{max}: intrinsic transmissivity on unit normal stress, 1 MPa.

$$T(\sigma_n, \Delta P, Q) = \theta(\sigma_n, \Delta P, Q) \cdot T_1^{max} \quad (3)$$

where T_1^{max} is the maximum value of transmissivity under a normal stress σ_n of 1 MPa. When the flow is not laminar, the transmissivity is a function of the flow and fluid pressure. This is why ΔP and Q appear in Eq. (3). The factor θ will vary from 1 (for $\sigma_n = 1$ MPa) to zero. Fig. 9 confirms the major influence of initial lateral displacement. Except for test 6AM, a greater normal stress is required for the samples with lateral displacement to obtain the same decrease of transmissivity (i.e. θ) as for the well matched samples.

4.2. Linear approximation of the behaviour

If we do not take into account the last stage of the test behaviour (large decrease in transmissivity or in θ for tests 5AM, 11AM and 12AM corresponding to the closure), it is possible to consider, as a first approximation, that the change in transmissivity is linear (on a semi-logarithmic scale). Thus, we can quantify the decrease of transmissivity and the difference between the samples with and without lateral displacement. A linear change in transmissivity on a logarithmic scale implies a relationship of the form: $\ln(T) = -\alpha \cdot \sigma_n + \beta$ with α and β being the slope and intercept respectively of the linear variation. Defining T^0 by e^{β}, it is possible to rewrite a simple law:

$$T = T_0 \cdot e^{-\alpha \cdot \sigma_n} \quad (4)$$

Parameters α and β, calculated for all hydromechanical responses, and both mean and standard deviation are summarized in Table 2. As mentioned earlier, tests with and without initial lateral displacement were treated separately. It has been found that if the sample has been subjected to an initial lateral displacement, then $\bar{\alpha} = 0.126$, while for cases of no lateral displacement $\bar{\alpha} = 0.542$. Thus, the difference in hydromechanical behaviour is quantified and there is a factor 4.3 between the average slopes of the two types of tests Indeed, a represents the ability of the interface to be closed. This factor becomes 4.8 if test 6AM is neglected.

Beyond the qualitative conclusion, this simple law provides a quantitative estimate of the influence of the initial lateral displacement on the hydromechanical behaviour.

4.3. Evaluation of the hydraulic aperture e_h

Many hydromechanical studies are based on the hydraulic and mechanical apertures of rock joints (Barton et al., 1985; Boulon et al., 1993; Esaki et al., 1999; Olsson and Barton, 2001). Fig. 10(a) shows the change in hydraulic aperture as a function of normal relative displacement.

Table 2
Coefficients α and β of the linear approximation of decrease of the intrinsic transmissivity of argillite–mortar interfaces in semi-logarithmic axis

Tests		Logarithmic scale $\ln(T) = -\alpha \cdot \sigma_n + \beta$		Normal scale $T = T_0 \cdot e^{-\alpha \cdot \sigma_n}$	$\bar{\alpha}$	Standard deviation	α_{max}	α_{min}
		α	β	$T_0 = e^{\beta}$				
With lateral displacement	2AM	0.076	−35.59	3.49E−16	0.126	0.04	0.184	0.076
	7AM	0.184	−35.66	3.25E−16				
	3AM	0.115	−34.87	7.18E−16				
	13AM	0.132	−32.73	6.1E−15				
Without lateral displacement	4AM	0.618	−35.46	3.98E−16	0.542	0.33	1.25	0.126
	6AM	0.126	−32.87	5.3E−15				
	1AM	0.447	−33.74	2.2E−15				
	5AM	0.353	−36.1	2.09E−16				
	8AM	1.250	−33.58	2.60E−15				
	9AM	0.610	−35.53	3.71E−16				
	11AM	0.208	−37	8.53E−17				
	12AM	0.339	−35.43	4.1E−16				

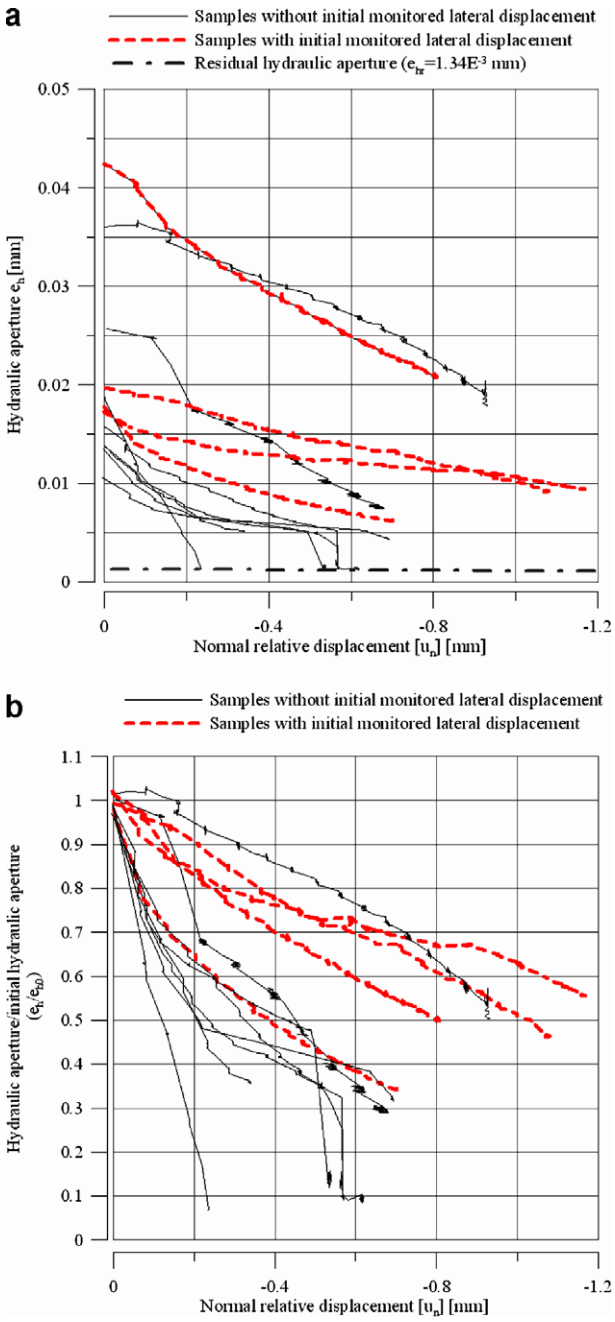

Fig. 10. (a) Evolution of hydraulic aperture (calculated by the cubic law) with respect to normal relative displacement. (b) Evolution of ratio hydraulic aperture/initial hydraulic aperture with respect to normal relative displacement.

This aperture is calculated using the cubic law ($T = e_h^3/12$ for the intrinsic transmissivity) and ranges from 1.3 μm (residual value when the interface is closed) to 45 μm. According to Witherspoon et al. (1980), the cubic law is valid within this range.

Hydraulic aperture decreases with increase in normal displacement. For well matched samples, this decrease is large at the beginning of the compression but the hydraulic aperture tends to a constant, no – zero value as compression is increased, as shown by Indraratna and Ranjith (2001). The change in hydraulic aperture is much more regular (almost linear) for the mismatched samples. Indeed, mismatching prevents the high closure at the beginning of compression that is seen with matched aperture faces. This difference between the two kinds of samples is more readable in Fig. 10(b) where the hydraulic aperture is divided by its initial value.

It is interesting to compare the variations of hydraulic aperture (Δe_h) induced by a variation of normal relative displacement ($\Delta[u_n]$) to this latter value. To consider more accurately the closure of the interface independently of the normal strain of the rock and concrete matrix, the normal relative displacement is corrected according to Eq. (5). This correction is established taking into account three sections of the samples subjected to a normal stress: i.e. the rock, the mortar and the interface (Fig. 11). The corrected normal displacement is expressed as

$$[u]_i = [u]_{total} - \sigma_n \cdot \left(\frac{h_m}{E_m} + \frac{h_r}{E_r}\right) \quad (5)$$

with:

- $[u]_i$: normal relative displacement of the interface,
- $[u]_{total}$: global measured normal relative displacement including rock and mortar matrices,
- h_m: height of the mortar part of lower section (5 mm),
- E_m: Young's modulus of the mortar (≈15 GPa),
- h_r: height of the argillite sample (maximum 65 mm),
- E_r: Young's modulus of the argillite (≈9 GPa),
- σ_n: normal stress.

Fig. 12 shows the change of the ratio $\frac{\Delta e_h}{|\Delta[u_n]|}$ with the corrected normal relative displacement. It is seen that the values are of the same order of magnitude for samples with and without lateral displacement – when a difference could have been expected. Moreover, $\frac{\Delta e_h}{|\Delta[u_n]|}$ quickly tends to very low values (about 0.01) meaning that reducing the hydraulic aperture becomes more and more difficult as normal stress increases. Many empirical relations have been proposed to link hydraulic and mechanical apertures (Barton et al., 1985; Benjelloun, 1991) but, while it is clear that an increase of normal relative displacement will decrease

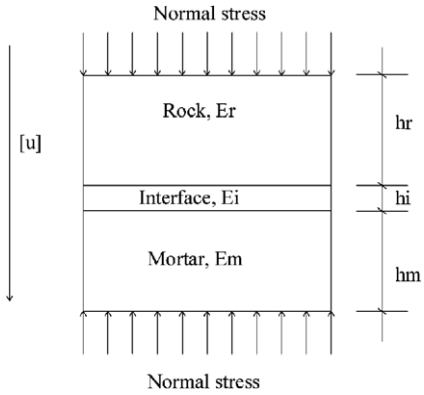

Fig. 11. Serial materials model. The three samples are subjected to a normal stress.

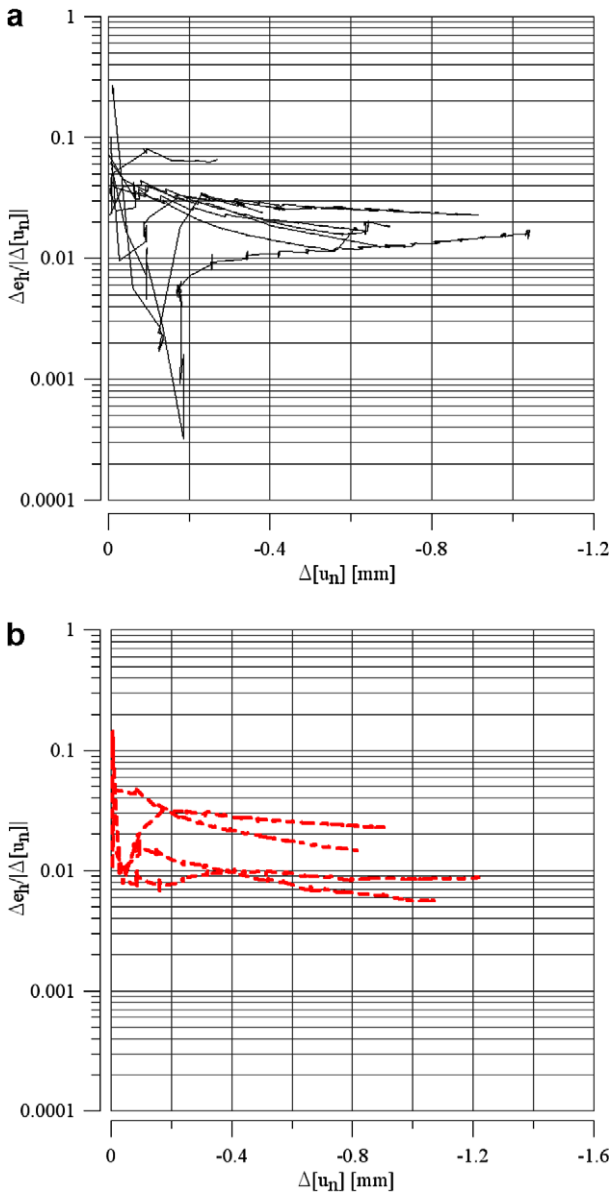

Fig. 12. Evolution of ratio ($\frac{\Delta e_h}{|\Delta[u_n]|}$) with respect to the variation of normal relative displacement: (a) samples without initial lateral displacement and (b) samples with initial lateral displacement.

the mechanical aperture (Barton et al., 1985; Hopkins et al., 1998; Chen et al., 2000), no data are available on the relation between $\Delta[u_n]$ and ΔE_m.

If we assume that $\Delta[u_n]$ and ΔE_m are of the same order of magnitude, we can compare our results to those of Barton et al. (1985). It appears than the ratio $\frac{\Delta e_h}{|\Delta[u_n]|}$ is less than the values determined by Barton (minimum value of 1/7). Moreover, this ratio is independent of the initial matching of the rock walls.

4.4. Validity of the transmissivity calculation

The calculation of the transmissivity is based on Darcy's law, assuming that the flow is laminar. If not, a kinetic term appears in the expression for the hydraulic gradient (v^2 in

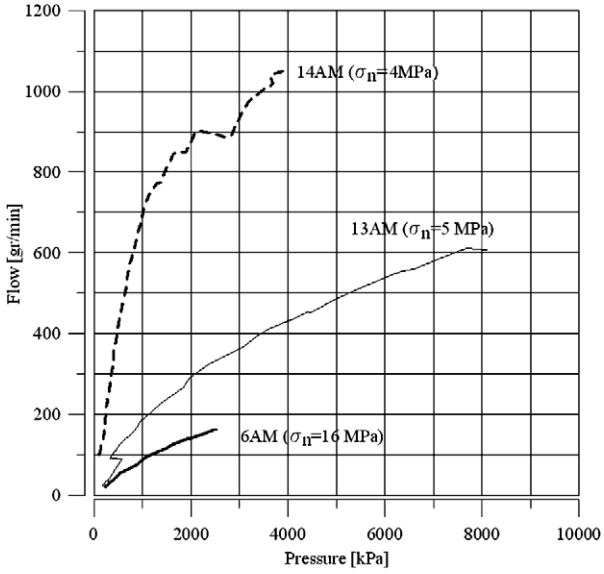

Fig. 13. "Hydraulic excursions" performed during tests 6AM, 13AM and 14AM for different values of normal stress.

Forcheimer's law or v^n with $n > 2$ (Rasoloarijaona, 1993)). To check the laminarity of the flow within the interfaces tested, some "hydraulic excursions" have been performed at different normal stresses for three tests. These "excursions" are presented in Fig. 13.

Pressure and flow have been increased from the initial hydraulic conditions and any deviation from a linear change going through the origin (equivalent to a constant transmissivity) means a loss of laminarity. The limits of laminarity, in terms of flow, are

- $Q \approx 100$ g/min for the test 6AM under 16 MPa (approximative Reynolds number $R_e = 220$),
- $Q \approx 100$ g/min for the test 13AM under 5 MPa (approximative Reynolds number $R_e = 200$),
- $Q \approx 500$ g/min for the test 14AM under 4 MPa (approximative Reynolds number $R_e = 1000$).

The Reynolds number, calculated at the inlet of the interface, is expressed as

$$R_e = \frac{2 \cdot Q}{\pi \cdot (r_i + e_h) \cdot v}$$

with:

- Q: water flow rate (m^3/s),
- r_i: internal radius (m),
- e_h: hydraulic aperture calculated by the cubic law (m),
- v: kinematic viscosity of the fluid (m^2/s).

In order to remain in the laminar domain and to verify the hypothesis of the Darcy's law, it is necessary to perform the hydromechanical tests with a low initial flow (about 100 g/min). Indeed, it is very difficult to determine accurately for each sample (and so for each void geometry), the laminar/turbulent transition value. In the case of turbu-

lent flow, the transmissivity becomes a function of pressure and flow rate (see Eq. (3)), increasing the natural dispersion. The quality of the tests and the relevance of the analysis are then affected.

5. Schematic application of the experimental results to the confinement by a concrete bulkhead

Let us consider a cylindrical concrete bulkhead in a gallery excavated in a geological massif of a specific stratification. We consider that the rock is locally damaged (EDZ of annular geometry Fig. 14). Moreover, a hydraulic gradient generates a flow from point A to point B. The data used are:

- diameter of the bulkhead: $D = 2R = 6$ m,
- thickness of the damaged rock equal to $1.2 \cdot R$, so $D_{EDZ} = 13.2$ m,
- range of permeability values for the geomaterials supposed homogeneous: $1E{-}21\ m^2 \leqslant K \leqslant 1E{-}17\ m^2$ (order of magnitude from the literature),
- hydraulic gradient between A and B: $i = -\mathrm{grad}(h)$,
- T: intrinsic transmissivity of the interface for a given level of normal stress (m^3),
- K_b: intrinsic permeability of the bulkhead (m^2),
- K_r: intrinsic permeability of the damaged rock (m^2).

Darcy's law is applied to this geometry to calculate the flows within the interface (Q_i), within the bulkhead (Q_b) and within the damaged rock (Q_r). Their expressions are

$$Q_b = K_b \frac{\gamma_w}{\mu} \cdot i \cdot \frac{\pi \cdot D^2}{4} \tag{6}$$

$$Q_i = T \cdot \frac{\gamma_w}{\mu} \cdot \pi \cdot D \cdot i \tag{7}$$

$$Q_r = K_r \frac{\gamma_w}{\mu} \cdot i \cdot \frac{\pi \cdot (D_{EDZ}^2 - D^2)}{4} \tag{8}$$

Then, two different ratios are defined:

$$\frac{Q_i}{Q_b} = \frac{4 \cdot T}{K_b \cdot D} \tag{9}$$

$$\frac{Q_i}{Q_r} = \frac{4 \cdot T \cdot D}{K_r \cdot (D_{EDZ}^2 - D^2)} \tag{10}$$

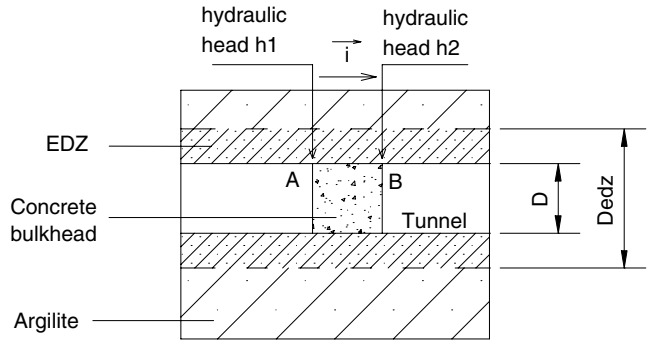

Fig. 14. Geometry of the application. A cylindrical concrete bulkhead is built in an excavated gallery.

The transmissivity T is calculated using the simple law defined equation 4($T = T_0 \cdot e^{-\alpha \cdot \sigma_n}$) but T_0, α and σ_n have to be chosen:

- we consider the maximum and minimum values found for the initial transmissivity ($T_0^1 = 1E-14\ m^3$ and $T_0^2 = 1E-16\ m^3$, see Table 2),
- we assume that $\alpha = 0.12$ (an in situ lateral relative displacement between the rock and the concrete cannot be avoided),
- We have chosen three steps of normal stress covering the expected range of stresses due to long term creep of the host rock: 0 MPa, 6 MPa and 12 MPa.

The corresponding values of T, which are summarized in Table 3, are used to calculate the ratios $\frac{Q_i}{Q_b}$ and $\frac{Q_i}{Q_r}$.

The change of these ratios with the permeability of the geomaterials is shown in Fig. 15. As the geomaterial permeability decreases, the ratios $\frac{Q_i}{Q_b}$ and $\frac{Q_i}{Q_r}$ increase. The curves of equal initial transmissivity for different normal stress are close to each other, which is due to the low value of α (i.e. the decrease of transmissivity as a function of time is very low). However, this analysis does not take into account phenomena affecting the materials: e.g. possible healing by calcite of the EDZ fractures or potential degradation by leaching of the concrete at the interface.

Concerning T_0, we have chosen extreme values of our results but we can expect values higher than $1E{-}14\ m^3$. Indeed, the in situ rock wall roughness (excavation by pneumatic hammer or blasting) may be larger than the artificial value used in the laboratory tests. The combination of a large roughness and lateral displacement of the interface will lead to higher transmissivity than the values obtained in the laboratory. Moreover, the scale effect, which tends to amplify any phenomenon, is not taken into account.

For classical values of rock and concrete permeability ($1E{-}19\ m^2 \leqslant K \leqslant 1E{-}21\ m^2$) and for the lower interface transmissivity, the minimum value of the ratios is 100, which means that, even for the tighter interface contact, the flow is localized within the interface. This observation emphasizes the finding that interfaces are critical for the long term effectiveness of the confinement system. Moreover, localized flow can generate a degradation of the concrete by leaching; this will increase the flow still further.

Table 3
Different values of transmissivity for three levels of normal stress and for two values of initial transmissivity, deduced from Table 2

Evolution law: $T = T_0 \cdot e^{-\alpha \cdot \sigma_n}$			
α	0.12		
σ_n (MPa)	0	6	12
T [m^3] ($T_0^1 = 1E-14\ m^3$)	1E−14	4.8E−15	2.3E−16
T [m^3] ($T_0^2 = 1E-16\ m^3$)	1E−16	4.8E−17	2.3E−18

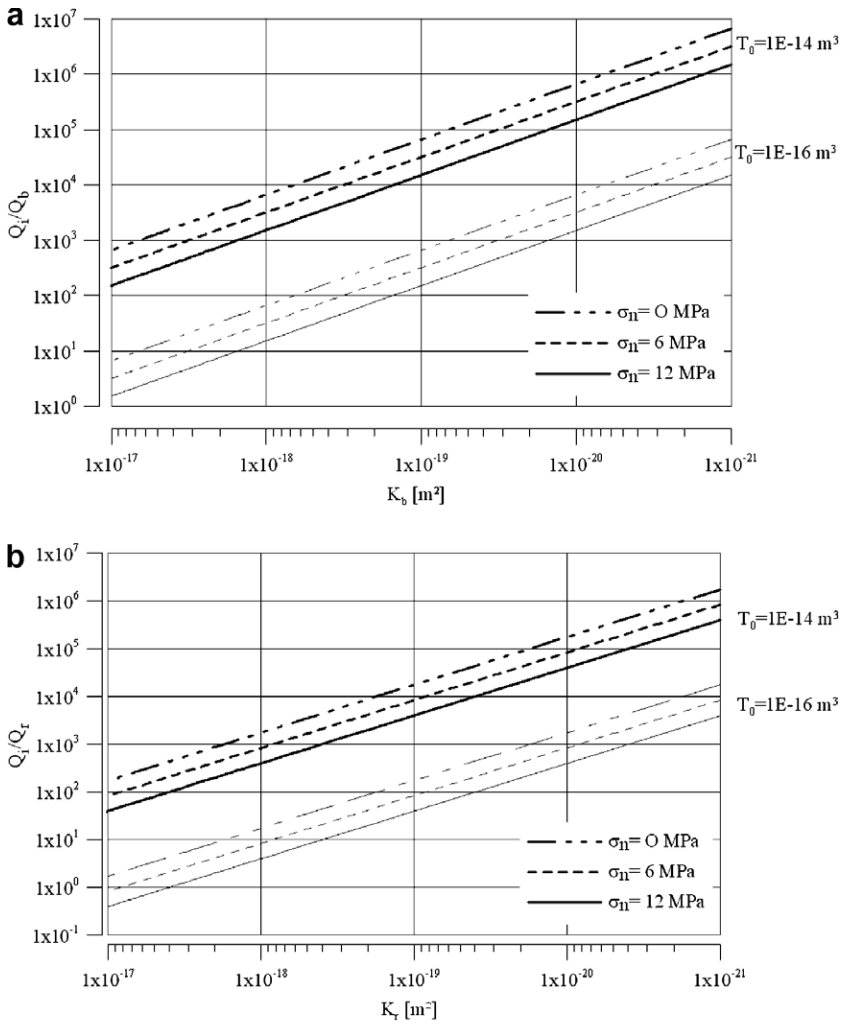

Fig. 15. Ratios $\frac{Q_i}{Q_b}$ (a) and $\frac{Q_i}{Q_r}$ (b) as a function of intrinsic permeability of the concrete or of the damaged rock, for three different levels of normal stress (0, 6 and 12 MPa) and for two values of initial transmissivity ($T_0^1 = 1\mathrm{E}-14\ \mathrm{m}^3$ and $T_0^2 = 1\mathrm{E}-16\ \mathrm{m}^3$).

6. Conclusions

This series of experiments was designed to investigate the influence of some specific variables of the rock–mortar interfaces, and intended to study realistic scenario for the behaviour of the interface between the concrete bulkhead and the rock. Shrinkage of the concrete bulkhead can result initially in a 'gap' at the interface, which will tend to close later due to long term creep of the host rock.

These tests have shown that such interfaces behave identically to rock joints from a qualitative hydraulic and mechanical point of view. The mechanical response of the interfaces is not affected by the investigated variables i.e. orientation of the bedding plane, effect of gravity and history of the contact. Even the initial lateral displacement of the interface has no significant effect, contrary to the observations by Bandis et al. (1983) who concluded that the stiffness of mismatched joints is lower than that of well-matched joints.

Some natural discontinuities corresponding to the rock bedding are present in the interface zone, perpendicular to the contact plane. Usually, geological water flows preferentially in such discontinuities compared to the rock mass but no increase of transmissivity was observed. By contrast, the change in transmissivity is modified considerably by an initial lateral displacement between faces of the interface. This lateral offset limits the aperture reduction and reduces the ability of the interface to close hydraulically. This finding is confirmed by an analysis of the hydraulic apertures based on the cubic law, which led to values of e_h much lower than classical values in the literature (Barton et al., 1985).

Moreover, the difference between samples with or without lateral displacement in terms of transmissivity has been quantified by a simple evolution law which is based on the parameter α, representing the decrease of transmissivity with normal stress. A factor 4.3 has been identified between the slopes of transmissivity decrease of the two kinds of

samples, highlighting the difference in hydromechanical behaviour ($\alpha_{\text{with LD}} = 4.3 \cdot \alpha_{\text{without LD}}$) between the two. Application of this law to the case of confinement by a concrete bulkhead, reveals the probability that flow will localize within the interface. This indicates that interfaces are critical for the efficiency of concrete seals, and points up the problem of material degradation (e.g. leaching of concrete). The true roughness of rock walls and scale effects have not been taken into account in the application discussed in the paper. These practical factors would lead to greater flow ratios than those calculated.

Finally, it has to be said that no major modification of the rock has been observed at the end of the tests despite the fact that the argillite is very sensitive to hydration/dehydration. It has been shown that rock surface variables do not have any major influence on the hydromechanical behaviour of the interfaces. Thus, these conclusions justify the use of 'rock surface replicates' in testing.

References

Armand, G. 2000. Contribution à la caractérisation en laboratoire et à la modélisation constitutive du comportement mécanique des joints rocheux. Ph.D. Thesis, Université Joseph Fourier, Grenoble, France.

Bandis, S.C., Lumsden, A.C., Barton, N.R., 1983. Fundamentals of rock joints deformation. Int. J. Rock Mech. Min. Sci. Geomech. Abstr. 20 (6), 249–268.

Barton, N., Bandis, S., Bakhtar, K., 1985. Strength deformation and conductivity coupling of rock joints. Int. J. Rock Mech. Min. Sci. Geomech. Abstr. 22 (3), 121–140.

Benjelloun, Z.H., 1991. Etude experimental et modélisation du comportement hydromécanique des joints rocheux. Ph.D. Thesis, Université Joseph Fourier, Grenoble and B.R.G.M, Orléans, France.

Boulon, M., 1995. A 3-d direct shear device for testing the mechanical behaviour and the hydraulic conductivity of rock joints. In: Proceedings of the MJFR-2 Conference, Vienna, Austria. Balkema, pp. 407–413.

Boulon, M., Selvadurai, A.P.S., Benjelloun, H., Feuga, B., 1993. Influence of rock joint degradation on hydraulic conductivity. Int. J. Rock Mech. Min. Sci. Geomech. 30, 1311–1317.

Capasso, G., Scavia, C., Gentier, S., Pellegrino, A., 1999. The influence of normal load on the hydraulic behaviour of rock fractures. In: ISRM Conference, Paris, pp. 863–868.

Charpentier, D., Tessier, D., Cathelineau, M., 2003. Shale microstructure evolution due to tunnel excavation after 100 years and impact of tectonic paleo-fracturing. case of tournemire, France. Eng. Geol. 70, 55–69.

Chen, Z., Narayan, S.P., Yang, Z., Rahman, S.S., 2000. An experimental investigation of hydraulic behaviour of fractures and joints in granitic rock. Int. J. Rock Mech. Min. Sci. 37, 1061–1071.

Daupley, X. 1997. Etude du potentiel de l'eau interstitielle d'une roche argileuse et de relations entre ses propriété hydriques et mécanique-application aux argilites du toarcien de la région de tournemire (aveyron). Ph.D. Thesis, Ecole Nationale Supérieure des Mines de Paris.

Didry, O., Gray, M.N., Cournut, A., Graham, J., 2000. Modelling the early age behavior of a low heat concrete bulkhead sealing an underground tunnel. Can. J. Civ. Eng. 27 (1), 112–124.

Direction scientifique, 2001. Service matériaux. Référentiel Matériaux. Tome 3: Les connaissances à l'échelle du secteur. Technical Report CRP.AMAT.01.060. ANDRA.

Dixon, D.A., Martino, J.B., Chandler, A., Sugita, Y., Vignal, B., 2002. Water uptake by a clay bulkhead installed in the tunnel sealing experiment at atomic energy of Canada's underground research laboratory. In: Clays in Natural and Engineered Barriers for Radioactive Waste Confinement. Experiments in Underground Laboratories. ANDRA.

Esaki, T., Du, S., Mitani, Y., Ikusada, K., Jing, L., 1999. Development of shear-flow test apparatus and determination of coupled properties for a single rock joint. Int. J. Rock Mech. Min. Sci. 36, 641–650.

Gale, J.E., Raven, R.G., 1985. Water flow in natural rock fracture as a function of stress and sample size. Int. J. Rock Mech. Min. Sci. Geomech., Abstr. 22 (4), 251–261.

Gangi, A.F., 1978. Variation of whole and fractured porous rock permeability with confining pressure. Int. J. Rock Mech. Min. Sci. Geomech. Abstr. 15, 249–257.

Gens, A., Guimaraes, L.doN., Garcia-Molina, A., Alonso, E.E., 2002. Factors controlling rock–clay buffer intercation in a radioactive waste repository. Eng. Geol. 64, 297–308.

Grindrod, P., Peletier, M., Takase, H., 1999. Mechanical interaction between swelling compacted clay and fractured rock, and the leaching of clay colloids. Eng. Geol. 54, 159–165.

Hans, J. 2002. Etude expérimental et modélisation numérique multiéchelle du comportement hydromécanique de répliques de joints rocheux. Ph.D. Thesis, Université Joseph Fourier, Grenoble, France.

Hans, J., Boulon, M., 2003. A new device for investigating the hydromecanical properties of rock joints. Int. J. Numer. Anal. Meth. Geomech. 27, 513–548.

Hopkins, D., Riss, J., Lamontagne, E., Gentier, S. 1998. Hydromechanical behavior of a fracture: how to understand the flow path. In: Proceeding of the MJFR-3 Conference, Vienna, Austria.

Indraratna, B., Ranjith, P., 2001. Hydromechanical Aspects and Unsaturated Flow in Jointed Rock. A.A. Balkema Publisher.

Johnston, I.W., Kodikara, J.K., 1994. Shear behaviour of irregular triangular rock–concrete joints. Int. J. Rock Mech. Min. Sci. Geomech. Abstr. 31 (4), 313–322.

Johnston, I.W., Lam, T.S.K., 1984. Frictional characteristics of planar concrete rock interfaces under constant normal stiffness conditions. In: Fourth Australia–New Zealand Conference on Geomechanics, Perth, 14–18 May, pp. 397–401.

Lee, H.S., Cho, T.F., 2002. Hydraulic characteristics of rough fractures in linear flow under normal and shear load. Rock Mech. Rock Eng. 35 (4), 299–318.

Mathieu, R., Pagel, M., Cklauer, N., De Windt, L., Cabrera, J., Boisson, J.Y., 2000. Paleofluids circulations records in shale: a mineralogical and geochemical study of calcite veions from experimental tournemire tunnel site (France).

Neville, A., 2000. Propriétés des bétons. Eyrolles.

Niandou, H., Shao, J.F., P Henry, J., Fourmaintraux, D., 1997. Laboratory investigations of the mechanical behaviour of the tournemire shale. Int. J. Rock Mech. Min. Sci. 34 (1), 3–16.

Olsson, R., Barton, N., 2001. An improved model for hydromechanical coupling during shearing of rock joints. Int. J. Rock Mech. Min. Sci. Geomech. Abstr. 38, 317–329.

Pusch, R., 1983. Stability of bentonite gel in crystalline rock – physical aspects. Technical Report TR-83-04, SKB.

Rasoloarijaona, M.N., 1993. on linéarités de la loi de darcy: étude théorique, numérique et expérimentale. Ph.D. Thesis, Université Joseph Fourier, Grenoble, France.

Rejeb, A., 1999. Mechanical characterisation of the argillaceous tournemire site (france). In: Site Characterisation Practice. Oxford & IBH Publishing Co. PVT. LTD., pp. 45–50.

Seidel, J.P., Haberfield, C.M., 2002. A theoretical model for rock joints subjected to constant normal stiffness direct shear. Int. J. Rock Mech. Min. Sci. 39, 539–553.

Witherspoon, P.A., Wang, J.S.Y., Iwai, K., Gale, J.E., 1980. Validity of the cubic law for fluid flow in a deformable rock fracture. Water Resour. Res. 16 (6), 1016–1024.